

CONF-7706112--1

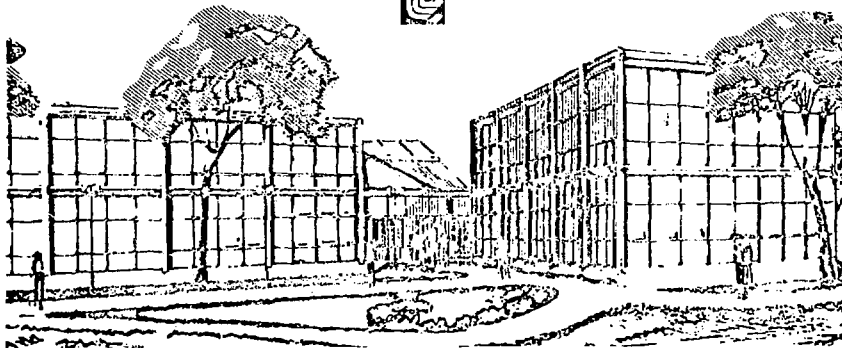
**Lawrence Livermore Laboratory**LASER-EXCITED FLUORESCENCE SPECTROSCOPY  
OF OXIDE GLASSES**MASTER**

M. J. Weber

June 1, 1977

This paper was prepared for Proceedings of the Seventh International Conference on Amorphous and Liquid Semiconductors, Edinburgh (June 27-July 1, 1977).

This is a preprint of a paper intended for publication in a journal or proceedings. Since changes may be made before publication, this preprint is made available with the understanding that it will not be cited or reproduced without the permission of the author.





In the next section, a brief survey is given of ion-glass interactions and major results of fluorescence line narrowing studies in glasses. (A more complete review and references to the original work are given in Ref. 1.) This is followed by recent results of laser-excited fluorescence spectroscopy in oxide glasses. Since FLN spectra are sensitive to the local structure, they can, in principle, be used to detect modifications of the probe ion environment arising from changes in the glass composition and from phase separation. Evidence of these effects are reported for alkali borate glasses. The use of transition metal ions other than the rare earths is then considered. Finally, measurements of site-dependent variations in the rate of nonradiative relaxation by multiphonon processes are presented.

## 2. Paramagnetic Ion - Glass Interactions

The Hamiltonian for a paramagnetic ion in a solid is given by

$$H = H_{e1} + H_{SO} + V, \quad (1)$$

where  $H_{e1}$  is the electrostatic interaction of the electrons,  $H_{SO}$  is the spin-orbit term, and  $V$  is the potential at the ion site due to its environment. For rare earths, which have thus far been the principal paramagnetic ions used for laser-excited fluorescence studies in glass,  $H_{e1} \gg H_{SO} \gg V$ . The interelectron repulsion term  $H_{e1}$  is described by the Racah parameters. When an ion is introduced into a solid, these phenomenological parameters are reduced from their free-ion values. This is the nephelauxetic effect. It shifts the free-ion states and causes differences in the frequency of optical transitions between SL multiplets. In a glass, these parameters may vary from site to site because of differences in the rare-earth coordination number, the rare earth-ligand ion distances, and the degree of covalent bonding. The result is inhomogeneous broadening of optical transitions.

The local field at the ion site in a glass is described by expanding the potential  $V$  in Eq. (1) in terms of tensor operators  $C_q^{(k)}$  that transform like spherical harmonics. Thus,

$$V = \sum_{k,q,i} B_q^k (C_q^{(k)})_i, \quad (2)$$

where the  $B_q^k$  are parameters to be determined from experimental data and the summation involving  $i$  is over all electrons of the ion of interest. The number and type of terms in Eq. (2) are derived from group theory given the site symmetry. If the site symmetry in the glass is very low ( $C_1$ ), all terms in Eq. (2) are possible. For  $f$  electrons,  $k$  is limited to values  $\leq 6$ .

The even- $k$  terms in Eq. (2) remove the degeneracy of the free-ion  $J$  states of rare earths and cause Stark splitting of  $\sim 10^2 \text{ cm}^{-1}$ . They also introduce admixing of  $J$  states but this is a smaller effect. Differences in the Stark splittings of FLN spectra as a function of excitation energy are related to differences in the local field parameters  $B_q^k$ .

M. J. Weber on  
LASER-EXCITED FLUORESCENCE SPECTROSCOPY OF OXIDE GLASSES

In a pioneering paper, Brecher and Riseberg<sup>2</sup> showed how distortions of a simple structural model of the first coordination shell yield predicted splittings that are consistent with the signs and relative magnitudes of the measured  $B_q^k$  parameters.

Radiative transition probabilities are also site-dependent. The odd- $k$  terms in Eq. (2) cause mixing of states of opposite parity. While small, it is this admixing which makes normally Laporte-forbidden electric-dipole transitions between levels of a given configuration possible. Since the  $B_q^k$  parameters and the interconfigurational radial integrals in the electric-dipole transition probability are dependent on the local environment, paramagnetic ions in glass exhibit a distribution of radiative decay rates. With broadband excitation and observation, the fluorescence from different sites is summed and the decay appears nonexponential. With laser excitation, the excited-state lifetimes of selected subsets of ions can be measured.

Paramagnetic ions interact with the local vibrations in glass. Nonradiative transitions between energy levels separated by less than the maximum phonon energy occur by direct and Raman relaxation processes. These one- and two-phonon mechanisms cause rapid transitions between Stark levels and lifetime broadening. The strength of the ion-host coupling and the resultant homogeneous broadening at individual ion sites varies because of differences in the separation of energy levels, local fields, and vibrational modes. Fluorescence line narrowing provides a method for studying homogeneous linewidths in glass<sup>3</sup> and variations in the ion-phonon coupling.

Selzer *et al.*<sup>4</sup> have demonstrated that line-narrowed fluorescence can also reveal the presence of other line-broadening mechanisms. Studies of a given rare-earth transition in oxide glasses and crystals at liquid-helium temperatures showed that the linewidth in the glass was significantly larger and had a different temperature dependence. The increased broadening in the glasses was attributed to motions associated with low-frequency excitations (tunneling or disorder modes) which, as evident from many other experiments, are present in amorphous materials at low temperatures.

When the concentration of paramagnetic ions is high, ion-ion interactions cause both spatial and spectral energy diffusion. By observing the time evolution of laser-excited fluorescence spectra, information has been obtained about energy transfer between dissimilar sites in inhomogeneously broadened systems.<sup>5,6</sup> Detailed analysis of the transfer process is complicated because, as we have seen, ions in different sites have different energy levels, transition probabilities, lineshapes, and linewidths. Added to this are considerations of the spatial distribution of sites and the relative importance of multipolar, exchange, and phonon-assisted processes. To avoid effects of cross relaxation, measurements of line-narrowed spectra are made by using small paramagnetic ion densities and observing the fluorescence immediately following the excitation pulse.

### 3. Alkali Borate Glasses

Two structural phenomena occur in binary alkali borate glasses which modify local site and are, in principle, detectable by fluorescence line narrowing. First, in simple  $B_2O_3$ , boron has three coordinating oxygens and a glass is formed from a random network

M. J. Weber on  
LASER-EXCITED FLUORESCENCE SPECTROSCOPY OF OXIDE GLASSES

of  $\text{BO}_3$  triangles. If an alkali oxide is added as a network modifier, boron also occurs with four coordinating oxygens in a tetrahedral complex. The relative numbers of three- and four-coordinated boron ions in alkali-borate systems have been determined from NMR studies. Second, subliquidus immiscibility is well established in binary alkali borates. Separation into  $\text{B}_2\text{O}_3$ -rich and lithia-rich phases occurs in regions on a scale of 5-500 nm. Therefore, if a paramagnetic ion is introduced into these glasses, the position of lines in the laser-excited fluorescence spectra should reflect differences in the number of nearby  $\text{BO}_3$  triangles,  $\text{BO}_4$  tetrahedra, and  $\text{Li}^+$  network-modifier cations. Evidence of these effects has been reported.<sup>7</sup>

Two lithium-borate glasses doped with 1 mol.%  $\text{Eu}_2\text{O}_3$  were studied: one with 40 mol.%  $\text{Li}_2\text{O}$ , a concentration at which the fractional number of borons with four coordinating oxygens is a maximum ( $\approx 45\%$ ), and a second with 10 mol.%  $\text{Li}_2\text{O}$ , which is at the maximum of the coexistence curve. Ions were excited into the  $^5\text{D}_0$  and  $^5\text{D}_2$  states of  $\text{Eu}^{3+}$  and the subsequent fluorescence from the  $^5\text{D}_0$  state to levels of the  $^7\text{F}$  multiplet was observed. The FLN spectra for the 40 $\text{Li}_2\text{O}$ -60 $\text{B}_2\text{O}_3$  glass recorded by J. Hegarty are shown in Fig. 1 (excitation energies are given at the left of each spectrum).

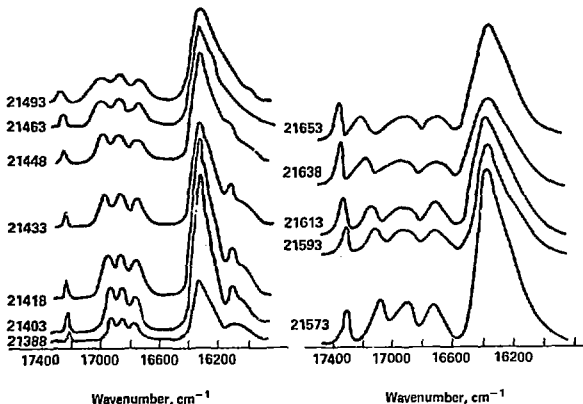


Fig. 1. Laser-excited fluorescence spectrum of  $\text{Eu}^{3+}$  in 40 $\text{Li}_2\text{O}$ ·60 $\text{B}_2\text{O}_3$  glass at 2 K as a function of  $^7\text{F}_0$  -  $^5\text{D}_2$  excitation energy ( $\text{cm}^{-1}$ ).

The  $^5\text{D}_0 + ^7\text{F}_0$  line appears in the region 17,000 - 17,400  $\text{cm}^{-1}$ , the three  $^5\text{D}_0 + ^7\text{F}_1$  transitions in the region 16,700-17,250  $\text{cm}^{-1}$ , and the five  $^5\text{D}_0 + ^7\text{F}_2$  transitions in the region 15,800-16,600  $\text{cm}^{-1}$ . The last group of lines is not well resolved. In general, transitions observed under nonresonant conditions exhibit residual inhomogeneous broadening because of accidental coincidence of excitation levels of ions in different sites.<sup>3,6</sup>

M. J. Heber on  
LASER-EXCITED FLUORESCENCE SPECTROSCOPY OF OXIDE GLASSES

The splitting of the  ${}^7F_1$  manifold displays a large variation with excitation energy. This is shown in Fig. 2 for excitation tuned across the  ${}^7F_0 \rightarrow {}^5D_0$  absorption line. Included in Fig. 2 are Drecher and Riseberg's results<sup>2</sup> for a sodium-barium-zinc silicate glass. The magnitude and pattern of the splittings, while not identical, are similar. This suggests the dominant role of the oxygen ligands, rather than the network-forming or network-modifying cations, in determining the local field at the  $\text{Eu}^{3+}$  site in oxide glasses.

Spectra for the  $10\text{Li}_2\text{O} \cdot 90\text{B}_2\text{O}_3$  glass is shown in Fig. 3. At low excitation energies, the spectra are nearly equal to those observed in the 40%  $\text{Li}_2\text{O}$  borate glass; at high excitation energies, however, the splittings are different and additional lines appear. Referring to the numbered lines on the spectrum at the top of Fig. 3, there are two groups of lines characterized by different fluorescence lifetimes. The first group consists of lines 1, 2, 5, 6, and 8 and has a shorter lifetime than the second group consisting of lines 3, 4, and 7.

Part of the inhomogeneous broadening of the  ${}^7F_0 \rightarrow {}^5D_0$  transition arises from the nephelauxetic effect. When the europium-oxygen interaction is large, the Racah parameters and the  ${}^7F - {}^5D$  separation are reduced. Thus, the low-excitation-energy spectra in Figs. 1 and 3 arise from ions in sites where the  $\text{Eu-O}$  interaction is strong. This occurs when there are many four-coordinated boron or lithium cations. Conversely, if three-coordinated borons predominate, the effective  $\text{Eu-O}$  interaction is weaker and the  ${}^7F_0 \rightarrow {}^5D_0$  transition occurs at higher energies. This suggests that the new lines appearing in the 10%  $\text{Li}_2\text{O}$  glass arise when  $\text{BO}_3$  triangles are more numerous.

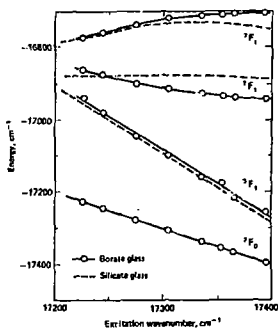


Fig. 2.  ${}^7F_1$  energy levels of  $\text{Eu}^{3+}$  in borate and silicate glasses as a function of the  ${}^7F_0 \rightarrow {}^5D_0$  excitation energy. The  ${}^5D_0$  level is taken as the zero of energy.



Fig. 3. Laser-excited fluorescence spectra of  $\text{Eu}^{3+}$  in  $10\text{Li}_2\text{O} \cdot 90\text{B}_2\text{O}_3$  glass at 2 K as a function of  ${}^7F_0 \rightarrow {}^5D_0$  excitation energy ( $\text{cm}^{-1}$ ).

Phase separation of binary alkali-borate systems has been analyzed in terms of one phase composed of a complex  $(B_2O_3)_m$  structure and another phase composed of a compound  $Li_2O \cdot nB_2O_3$ .<sup>8</sup> When phase separation occurs, it is not known whether an ion such as  $Eu^{3+}$  goes into one or both phases. The 40%  $Li_2O$  borate glass represents a lithia-rich phase. To identify a  $B_2O_3$ -rich phase, studies of  $Eu^{3+}$  in simple  $B_2O_3$  glass are needed. Attempts to add  $Eu_2O_3$  to  $B_2O_3$  have had only limited success.

The above results and their interpretation are still incomplete. Further studies are needed in which the alkali ion is changed and the alkali ion concentration varied between the minimum and maximum possible. The effects of phase separation should be investigated as a function of thermal history. The resulting spectroscopic parameters should provide a test of geometric models for the local coordination at the probe ion site.

#### 4. Ions for Fluorescence Line Narrowing

Trivalent rare earths have been used almost exclusively for laser-excited fluorescence studies in glass. These ions possess the desirable properties of small homogeneous linewidths for f-f transitions and local fields which can be treated as small perturbations, but the energy-level schemes are complicated by the large number of Stark levels.

Laser-induced fluorescence line narrowing in solids was first demonstrated for  $Cr^{3+}$  in ruby where the narrow  ${}^2E \rightarrow {}^4A_2$  R-line fluorescence was studied. In most oxide glasses, the cubic crystal-field parameter  $Dq$  describing the local field at the  $Cr^{3+}$  site is smaller and the energy levels are ordered as shown in the Tanabe-Sugano energy level diagram, Fig. 4. Broadband  ${}^4T_2 \rightarrow {}^4A_2$  emission rather than  ${}^2E \rightarrow {}^4A_2$  emission dominates. The large homogeneous width ( $\sim 10^3 \text{ cm}^{-1}$ ) of this transition masks site-to-site variations in the local fields. Such variations are evident, however, from the non-exponential fluorescence decay. Whereas laser excitation into  ${}^4T_2$  generally produces no significant line narrowing, some site selectivity can be obtained by exciting into the long-wavelength tail of the  ${}^4A_2 \rightarrow {}^4T_2$ ,  ${}^2E$  absorption band.<sup>9</sup>

Line emission from other transition and post-transition metal ions in glasses suitable for line narrowing is rare. One seeks pairs of levels with separations which are independent of the crystal field. Examples of electronic configurations, ions, and transitions which have this characteristic are  $d^2(V^{3+})$ :  ${}^3T_1 - {}^1T_2$ ;  $d^3(Cr^{3+}, Mo^{3+})$ :  ${}^4A_2 - {}^2E$  and  ${}^4A_2 - {}^2T_2$ ;  $d^6(Mn^{2+}, Fe^{3+})$ :  ${}^6S - {}^4G$ ; and  $d^8(Ni^{2+})$ :  ${}^3A_2 - {}^1E$ .

Although  $Cr^{3+}(3d^3)$  is of limited usefulness, its  $4d^3$  counterpart,  $Mo^{3+}$ , is a candidate of line narrowing. The optical spectra of  $Mo^{3+}$  in oxide glasses has been investigated by Parke and co-workers.<sup>10</sup> As shown in Fig. 4, the crystal-field parameter is much larger for  $4d$  electrons ( $Dq \approx 2200 \text{ cm}^{-1}$  for  $Mo^{3+}$  versus  $\approx 1600 \text{ cm}^{-1}$  for  $Cr^{3+}$ ) and the first excited state is  ${}^2E$ .

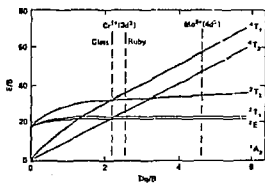


Fig. 4. Energy levels of the  $d^3$  electronic configuration.

M. J. Weber on  
LASER-EXCITED FLUORESCENCE SPECTROSCOPY OF OXIDE GLASSES

The  ${}^2E \rightarrow {}^4A_2$  fluorescence spectrum of  $\text{Mo}^{3+}$  in a phosphate glass at 77 K is shown in Fig. 5. Laser-induced line narrowing has been observed, but the oscillator strength of the transition is small and the  $\text{Mo}^{3+}$  concentrations achievable thus far have been low, ~ 0.2 mol.%  $\text{MoO}_3$ .

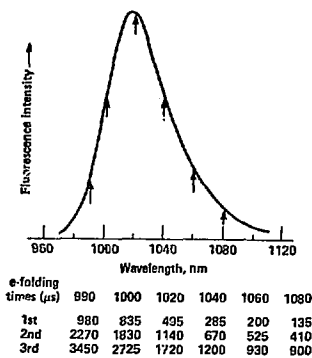


Fig. 5.  ${}^2E \rightarrow {}^4A_2$  fluorescence spectrum and fluorescence lifetimes as a function of wavelength for  $\text{Mo}^{3+}$  in phosphate glass at 77 K.

The linewidths of the  ${}^4A_2 \rightarrow {}^2E$  transition for  $\text{Cr}^{3+}$  or  $\text{Mo}^{3+}$  in glasses are very much larger than in crystals. This is due in large part to the site dependence of the nephelauxetic effect. In the strong field limit, the  ${}^4A_2 \rightarrow {}^2E$  separation is independent of  $Dq$  and is given by  $9B + 3C$ , where  $B$  and  $C$  are the Racah parameters. The nephelauxetic effect is more pronounced for 3d and 4d electrons of  $\text{Cr}^{3+}$  and  $\text{Mo}^{3+}$  than for 4f electrons of the rare earths. For example, whereas the free-ion value of  $B$  for  $\text{Cr}^{3+}$  is  $920 \text{ cm}^{-1}$ , in solids it has a value ~  $600\text{-}700 \text{ cm}^{-1}$ .

### 5. Multiphonon Processes

When the energy difference between an excited state and the next-lower level exceeds the single phonon energy, multiphonon processes are required to conserve energy in a purely nonradiative transition. The larger the energy gap, the more phonon required and the less probable the process. Studies of nonradiative relaxation of excited rare earths in crystals and glasses have shown that for a given rare earth and host, the rates of these high-order processes are determined principally by the size of the energy gap rather than the particular electronic states or phonon modes involved. For different hosts, the phonon spectrum and strength of the ion-phonon coupling may vary. The dependence of multiphonon relaxation rates on the phonon spectrum was recently demonstrated for a series of oxide glasses (borate, phosphate, silicate, germanate, tellurite) with progressively smaller phonon energies.<sup>11</sup>

As mentioned earlier, the ion-phonon interaction in glasses is also site-dependent. This is reflected in the range of homogeneous linewidths observed in FLN experiments and in the rates of multiphonon relaxation of rare earths. For example, the relaxation of the  ${}^4S_{3/2}$  state of  $\text{Eu}^{3+}$  in glasses is predominantly by multiphonon emission to  ${}^4F_{9/2}$ . For non-selective excitation, this decay in a beryllium fluoride glass is nonexponential with rates varying by a factor of 2.5.

Using laser-excited fluorescence, site-dependent variations in the transition probabilities of rare earths in glass have been reported by Brecher *et al.*<sup>12</sup>



The glass was neodymium silicate laser glass, ED-2. Using a tunable dye laser, ions were excited into the  ${}^2P_{1/2}$  state followed by rapid decay to the  ${}^4F_{3/2}$  state from which fluorescence was observed to the  ${}^4I$  ground multiplet. With pulsed laser excitation, the resulting fluorescence decay was exponential with a lifetime which varied with excitation wavelength as shown in Fig. 6. Since the fluorescence lifetime is given by

$$1/\tau = 1/\tau_R + 1/\tau_{NR},$$

where  $\tau_R$  and  $\tau_{NR}$  are the lifetimes for radiative and nonradiative decay, the variation in Fig. 6 can arise from one or both processes. To determine  $\tau_R$ , the fluorescence intensity was measured under conditions of constant absorbed excitation into  ${}^2P_{1/2}$ . The radiative quantum efficiency  $\eta = \tau/\tau_R$  was then normalized to unity at one wavelength and the resulting variations in  $\tau_R$  and  $\tau_{NR}$  plotted in Fig. 6. Similar experiments with  $\text{Nd}^{3+}$  in fluoride glass showed no variation in  $\eta$  because the ion-phonon interaction is weaker and multiphonon relaxation is negligible. In contrast, in borate glasses the phonon frequencies are larger and the  ${}^4F_{3/2}$  level of  $\text{Nd}^{3+}$  decays predominantly by multiphonon emission. Measurements of site-dependent transition probabilities in a series of fluoride, silicate, phosphate, and borate glasses are in progress.<sup>13</sup>

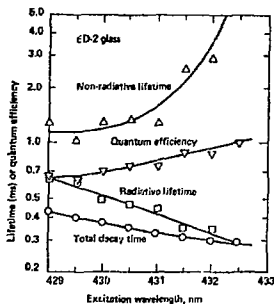


Fig. 6. Relative quantum efficiency and lifetimes of the  $\text{Nd}^{3+}$  fluorescence in ED-2 silicate glasses at  $\sim 15$  K as a function of the  ${}^4I_{9/2} + {}^2P_{1/2}$  excitation wavelength. The quantum efficiency is normalized to unity at 432.5 nm.

A more dramatic variation of multiphonon decay rates is observed for the  ${}^2E \rightarrow {}^4A_2$  transition of  $\text{Mo}^{3+}$  in phosphate glass.<sup>14</sup> The energy gap is large,  $\approx 10,000 \text{ cm}^{-1}$ , but the ion-phonon coupling for the outer 4d electrons of  $\text{Mo}^{3+}$  is greater than for the shielded 4f electrons of rare earths. The spin-orbit interaction admixes states to remove the spin forbiddenness of the  ${}^4A_2 \rightarrow {}^2E$  transition. From the  ${}^4A_2 \rightarrow {}^2E$  absorption intensity, the average radiative lifetime of the  ${}^2E$  state is estimated to be  $\sim 5$  ms.<sup>10</sup> For broadband excitation into the  ${}^4T$  bands, the fluorescence decay is very nonexponential with initial and final decay rates differing by about one order of magnitude at both 300 and 77 K. Using a monochromator to observe the decay at selected wavelengths, DeGroot measured the lifetimes shown in Fig. 5. The variation from the fastest to the slowest e-folding times was  $\approx 25$ . Since all the decay rates are temperature-dependent and at low temperatures are less than the predicted radiative rate, the decay is attributed to nonradiative processes.

Multiphonon processes for transition metal ions have been treated by Sturge.<sup>15</sup> These higher-order processes are very dependent upon the anharmonicity of the interaction

M. J. Weber on  
LASER-EXCITED FLUORESCENCE SPECTROSCOPY OF OXIDE GLASSES

and the energy gap. From the inhomogeneous broadening in Fig. 5, ions are present in sites with energy gaps varying by  $\sim 1000 \text{ cm}^{-1}$  or 10% of  ${}^2E \rightarrow {}^4A_2$ . The range of observed decay rates is similar to that expected from the gap dependence of multiphonon processes. Nonradiative decay by ion-ion energy transfer is ruled out because the  $\text{Mo}^{3+}$  ion density was small,  $\sim 10^{19}/\text{cm}^3$ , and the ions with the largest energy level separations have the longest lifetimes, in contrast to the expected migration to the lowest energy states.

The longest lifetimes are observed for ions having the largest  ${}^2E \rightarrow {}^4A_2$  separation. These are also the ions which have the largest Racah parameters B and hence the smallest covalency. To explore the relationship between covalency and strength of ion-phonon coupling, tunable pulsed lasers are being used to selectively excite ions within the  ${}^4A_2 \rightarrow {}^2E$  absorption profile. The resulting variation of the multiphonon decay rates and their temperature dependence should provide additional insight into multiphonon processes for transition metal ions in oxide glasses.

#### Acknowledgments

I am grateful to the following people for results presented in this paper: Drs. J. Hegarty and H. M. Yen of the University of Wisconsin for the lithium borate glass studies; Drs. C. Brecher and L. A. Riseberg of GTE Laboratories for the investigation of site-dependent transition probabilities of neodymium; and Dr. C. B. Layne and A. J. DeGroot of the Lawrence Livermore Laboratory for the measurements of rare-earth multiphonon relaxation and fluorescence properties of  $\text{Mo}^{3+}$ , respectively. Glasses used in these studies were prepared by D. H. Blackburn of the National Bureau of Standards and J. D. Myers of Kigre, Inc.

#### References

1. M. J. Weber, in Proc. Colloque de Lyon, J. Phys. (Paris), in press.
2. C. Brecher and L. A. Riseberg, Phys. Rev. B13, 81 (1976).
3. T. Kushida and E. Takushi, Phys. Rev. B12, 824 (1975).
4. P. M. Seizer, D. L. Huber, D. S. Hamilton, H. M. Yen, and M. J. Weber, Phys. Rev. Lett. 36, 813 (1976).
5. N. Motegi and S. Shionoya, J. Luminescence 8, 1 (1973).
6. M. J. Weber, J. A. Paisner, S. S. Sussman, H. M. Yen, L. A. Riseberg, and C. Brecher, J. Luminescence 12, 729 (1976).
7. M. J. Weber, J. Hegarty, and D. H. Blackburn, in Boron in Glass and Glass Ceramics (Plenum Press, New York), in press.
8. P. B. Macedo and J. H. Simmons, J. Res. Nat. Bur. of Stds. 78A, 53 (1974).
9. S. A. Brauer and W. B. White, J. Chem. Phys. (1977), in press.
10. S. Parke, S. Gomoika, and J. N. Sandoe, J. Non-Cryst. Solids 20, 1 (1976).
11. C. B. Layne, H. H. Lowdermilk, and M. J. Weber, Phys. Rev. B16 (July 1977).
12. C. Brecher, L. A. Riseberg, and M. J. Weber, Appl. Phys. Lett. 30, 475 (1977).
13. C. Brecher (private communication).
14. M. J. Weber and A. J. DeGroot, Bull. Amer. Phys. Soc. 22, 466 (1977).
15. M. D. Sturge, Phys. Rev. B8, 6 (1973).

#### NOTICE

"This report was prepared as an account of work sponsored by the United States Government. Neither the United States nor the United States Energy Research & Development Administration, nor any of their employees, nor any of their contractors, subcontractors, or their employees, makes any warranty, express or implied, or assumes any legal liability or responsibility for the accuracy, completeness or usefulness of any information, apparatus, product or process disclosed, or represents that its use would not infringe privately-owned rights."

Reference to a company or product name does not imply approval or recommendation of the product by the University of California or the U.S. Department of Energy to the exclusion of others that may be suitable.